

SEPARATION OF NON-PERIODIC AND PERIODIC 2D PROFILE FEATURES USING B-SPLINE FUNCTIONS

Dariusz Janecki, Leszek Cedro, Jarosław Zwierzchowski

Kielce University of Technology, Faculty of Mechatronics and Machinery Design, Al. 1000-lecia P. P. 7, 25-314 Kielce, Poland
(✉ djanecki@tu.kielce.pl, +48 41 342 4444, lcedro@tu.kielce.pl, j.zwierzchowski@tu.kielce.pl)

Abstract

The form, waviness and roughness components of a measured profile are separated by means of digital filters. The aim of analysis was to develop an algorithm for one-dimensional filtering of profiles using approximation by means of B-splines. The theory of B-spline functions introduced by Schoenberg and extended by Unser et al. was used. Unlike the spline filter proposed by Krystek, which is described in ISO standards, the algorithm does not take into account the bending energy of a filtered profile in the functional whose minimization is the principle of the filter. Appropriate smoothness of a filtered profile is achieved by selecting an appropriate distance between nodes of the spline function. In this paper, we determine the Fourier transforms of the filter impulse response at different impulse positions, with respect to the nodes. We show that the filter cutoff length is equal to half of the node-to-node distance. The inclination of the filter frequency characteristic in the transition band can be adjusted by selecting an appropriate degree of the B-spline function. The paper includes examples of separation of 2D roughness, as well as separation of form and waviness of roundness profiles.

Keywords: profile filtering, B-spline functions, roundness, roughness.

© 2015 Polish Academy of Sciences. All rights reserved

1. Introduction

Smoothing and low-pass filtration of measurement data are performed in many areas of science and technology. In surface metrology, filtration is used to separate form, waviness and roughness components. Today, the most common are digital filters, because of application of computer-based measurement methods. The problem of filtration can be easily solved in the analysis of periodic profiles registered at a constant sampling interval. In this case, the most convenient is first to determine a discrete Fourier transform of a profile, and then filter it in the frequency domain according to the required filter frequency characteristic. Filtering non-periodic profiles is definitely more difficult. The major problem is to determine the filtered profile at the end points of the profile. This is due to the fact that the value of the filtered profile at a given point is obtained through averaging of the measured profile in a certain neighborhood of this point. However, at the ends of the profile, the values of the profile lying outside the area measured are not known. In the literature, this problem is called the end problem.

The simplest method to solve the problem is to register a sufficiently long fragment of a profile and use additional end fragments for determining the filtered profile in its central part. Many methods have been developed to determine a filtered profile, also at the profile ends [1–10]. Many of them have good theoretical background. In [1, 2], a variational approach was used. It assumes that the filtered profile minimizes a certain functional made up of two parts. One part is responsible for approximation of the primary profile by the filtered profile, whereas the other, called the bending energy, is meant to ensure appropriate smoothness of the filtered profile. In [3], the variational approach has been extended to the two-dimensional case. In [4, 5], a filtered profile is determined by means of local approximation of the primary profile with

a polynomial of degree 1 or higher. In the literature, such filters are called spline and regression filters, respectively, and they are described in ISO standardization documents [6, 7]. In [8], the Gaussian regression filter is compared with the spline filter. It was shown that, in certain cases, the performance of the regression filter was better than that of the spline filter.

There also exist other methods, more heuristic in nature. For instance, it is possible to adjust the profile inclination, so that the values at its both ends are equal, and then to treat the profile as a periodic one [9]. In [10], a profile was extrapolated by means of central symmetry with centers at the end points of the profile. The heuristic methods sometimes provide expected results, and sometimes fail. This implies the occurrence of the end effect, which manifests in a considerable deviation of the filtered profile from the expected values at profile ends.

Data smoothing can also be achieved by approximating the profile by a linear combination of certain basis functions φ_k , *i.e.*, by means of the sum $\sum_{k=0}^{K-1} a_k \varphi_k(t)$, where t is a spatial variable. Typically, the approximation is performed using a partial sum of the Fourier series. This method is used mainly for periodic profiles. In this paper, we assumed that the basis functions were appropriately shifted B-spline functions (B-splines). We used the theory of B-spline functions developed by Schoenberg [11] and extended by Unser *et al.* [12]. We formulated the problem of approximation of measuring data by means of periodic and non-periodic B-spline functions and discussed the properties of the resulting low-pass filter. We included examples of application of the filter to separate 2D roughness and to separate form and waviness of roundness profile.

It should be emphasized that, unlike spline filters described in the standard, the algorithm does not take into account the bending energy of the filtered profile in the functional whose minimization is the principle of the filter. The approximating function is smoothed by selecting an appropriate distance between nodes of the spline function.

2. Approximation of non-periodic function by means of B-spline functions

2.1. B-spline functions

Consider an interval $\mathcal{P} = [0, T_f]$ of a variable t . Assume that the interval is divided into K subintervals having the same length T . Then, the n -th degree spline function determined over the interval $t \in \mathcal{P}$ is a function $s(t)$ with the following properties:

- the function $s(t)$ is a function of class C^{n-1} , *i.e.*, it has a continuous derivative of order $n-1$;
- in the subintervals $t \in [kT, (k+1)T]$, $k = 0, 1, \dots, K-1$, the function $s(t)$ is a polynomial of a degree not higher than n .

The points kT , $k = 1, 2, \dots, K-1$ are called nodes of the spline function, whereas the parameter T is the distance between the nodes. Let us further assume that $x_m = x(t_m)$, $m = 1, 2, \dots, M$ is a sequence of values of a certain function $x(t)$ determined over the interval \mathcal{P} . In surface metrology, the function $x(t)$ can be regarded as a profile of a certain object, while the set of pairs (t_m, x_m) is the set of measuring points. The set of coordinates t_m can be distributed, uniformly or non-uniformly, over the interval \mathcal{P} . In the first case, we say that the values of the function $x(t)$ were obtained by applying a constant sampling interval.

The problem of approximation of the set of points (t_m, x_m) by means of a spline function can be formulated as follows: determine the spline function $s(t)$ that minimizes the functional:

$$J = \sum_{m=1}^M (x_m - s(t_m))^2 . \tag{1}$$

Note, that the functional (1) depends on the parameters of the spline functions. The number of these parameters is equal to $(n+1)K$, where, recall, $n+1$ is the number of coefficients of the n -th degree polynomial, while K is the number of subintervals of the interval \mathcal{P} . Since $s(t)$ is a function of class C^{n-1} , in each of the $K-1$ nodes within the interval \mathcal{P} , we can formulate n equations for the derivatives from order 0 to order $n-1$ for the polynomials adjacent to a given node. Thus, by eliminating the variables, the functional (1) can be made dependent on $K+n$ independent parameters.

A very convenient and elegant method for constructing spline functions is to apply B-spline functions (B-splines, for short) [11, 12]. B-splines can be defined in a few ways. The definition provided below is a recursive definition using the concept of convolution. Let $\hat{\beta}_0(t)$ be a characteristic function of the interval $[-1/2, 1/2]$, that is:

$$\hat{\beta}_0(t) = \begin{cases} 1 & \text{for } |t| \leq 1/2, \\ 0 & \text{otherwise,} \end{cases} \tag{2}$$

and assume that:

$$\hat{\beta}_n(t) = \hat{\beta}_{n-1}(t) * \hat{\beta}_0(t) \text{ for } n = 1, 2, \dots \tag{3}$$

For example, a cubic B-spline function, which is commonly applied, is described with the following relationship:

$$\hat{\beta}_3(t) = \frac{1}{6} \begin{cases} t^3 + 6t^2 + 12t + 8 & \text{for } -2 \leq t \leq -1, \\ -3t^3 - 6t^2 + 4 & \text{for } -1 \leq t \leq 0, \\ 3t^3 - 6t^2 + 4 & \text{for } 0 \leq t \leq 1, \\ -t^3 + 6t^2 - 12t + 8 & \text{for } 1 \leq t \leq 2, \\ 0 & \text{otherwise.} \end{cases} \tag{4}$$

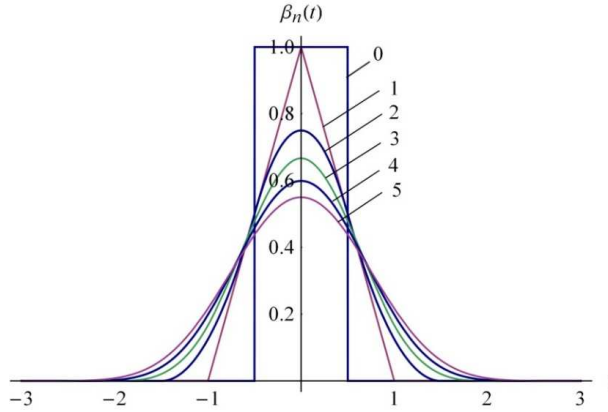
A B-spline function have many interesting properties. For instance, it is an even function, *i.e.*, $\hat{\beta}_n(t) = \hat{\beta}_n(-t)$, and is equal to zero for $t \geq (n+1)/2$. Moreover, from the definition (3), it follows that:

$$\hat{\beta}_n(t) = \underbrace{\hat{\beta}_0(t) * \hat{\beta}_0(t) * \dots * \hat{\beta}_0(t)}_n . \tag{5}$$

Thus, from the central limit theorem it is clear that for high values of n , the B-spline function resembles a Gaussian function:

$$\hat{\beta}_n(t) \cong \sqrt{\frac{6}{\pi(n+1)}} e^{-\frac{6t^2}{(1+n)}} . \tag{6}$$

Figure 1 shows a plot of the B-spline functions for several initial values of n .

Fig. 1. B-spline functions for $n = 0, 1, 2, 3, 4, 5$.

It is easy to check that the B-spline function $\hat{\beta}_n(t)$ is a spline function of degree n , with the node-to-node distance $T = 1$. The node coordinates are equal to $\dots, -2, -1, 0, 1, 2, \dots$ for odd n , and $\dots, -3/2, -1/2, 1/2, 3/2, \dots$ for even n . Therefore, the function $\hat{\beta}_n(t)$ is also called a normalized B-spline function. The B-spline function with an arbitrary node-to-node distance T is a function in the form:

$$\beta_{n,T}(t) = \frac{1}{T} \hat{\beta}_n(t/T). \quad (7)$$

Each n -th degree spline function determined over the interval $\mathcal{P} = [0, T_f]$ with its nodes at the points kT , $k = 1, 2, \dots, K-1$ can be written as:

$$s(t) = \begin{cases} \sum_{k=-(n-1)/2}^{K+(n-1)/2} a_k \beta_{n,T}(t-kT) & \text{for odd } n, \\ \sum_{k=-n/2}^{K+n/2-1} a_k \beta_{n,T}(t-kT-T/2) & \text{for even } n. \end{cases} \quad (8)$$

The summation range in the (8) was selected in such a way that the shifted basis functions in the (8) had non-zero values in the interval \mathcal{P} . Thus, for instance, for $n = 3$, the functional (1) can be written as:

$$J = \mathbf{a}^T \mathbf{B} \mathbf{a} - 2\mathbf{c}^T \mathbf{a} + d, \quad (9)$$

where d is a scalar, independent of the coefficients a_k , and:

$$\mathbf{a} = [a_{-1} \ a_0 \ \dots \ a_{K+1}]^T, \quad (10)$$

$$\boldsymbol{\beta}(t) = [\beta_{3,T}(t+T) \ \beta_{3,T}(t) \ \dots \ \beta_{3,T}(t-(K+1)T)]^T, \quad (11)$$

$$\mathbf{B} = \sum_{m=1}^M \boldsymbol{\beta}(t_m) \boldsymbol{\beta}(t_m)^T, \quad \mathbf{c} = \sum_{m=1}^M \boldsymbol{\beta}(t_m) x(t_m). \quad (12)$$

Finally, the parameters of the spline function which ensures the best approximation of the measuring points (t_m, x_m) in the sense of a minimum of (1) are as follows:

$$\mathbf{a} = \mathbf{B}^{-1} \mathbf{c}. \quad (13)$$

Now, it is essential to determine how to select the distance between nodes of the spline function, T . It is understandable that the greater the distance between nodes, the smoother the spline curve. Probably, the smoothness of the curve is also dependent on the degree n . The representation $(t_m, x_m) \rightarrow s(t)$ can be treated as a low-pass filter. Another important objective is to answer the question what the cutoff frequency of the defined filter is.

2.2. Properties of the filter using B-spline approximation

The properties of the filter were analyzed using a Fourier transform. For this purpose, let us consider the interval over which the spline function is defined. We assume that the approximated function is defined on the whole set of real numbers, *i.e.*, $\mathcal{P} = \mathbf{R}$. Moreover, the sampling period is constant and much smaller than the distance between nodes of the spline function, T . Now, we can assume that the approximated function $x(t)$ is continuous. Accordingly, the approximation can be performed by first finding a minimum of the functional:

$$J = \int_{-\infty}^{\infty} (x(t) - s(t))^2 dt \quad (14)$$

with respect to the parameters of the spline function:

$$s(t) = \sum_{k=-\infty}^{\infty} a_k \beta_{n,T}(t - kT). \quad (15)$$

The mapping $x(t) \rightarrow s(t)$ defined by the minimum of the functional (14) is a spatially-varying linear system. It can be described with an integral equation:

$$s(t) = \int_{-\infty}^{\infty} x(\Delta) h_{\Delta}(t - \Delta) d\Delta, \quad (16)$$

where $h_{\Delta}(t - \Delta)$ is the system response to a shifted Dirac impulse function $\delta(t - \Delta)$. (In other words, the function $h_{\Delta}(t)$ is a response of a system in which nodes of the spline function are shifted by $-\Delta$).

Proposition: The function $h_{\Delta}(t)$ has the following properties:

- 1) the functions $h_{\Delta}(t)$ and $h_{T/2}(t)$ are even functions;
- 2) the function $h_{\Delta}(t)$ is a periodic function with respect to the variable Δ with a period T ;
- 3) the Fourier transform of the function $h_{\Delta}(t)$ as a function of the variable t is:

$$H_{\Delta}(\omega) = \hat{\mathbf{B}}_n(\omega T) \frac{\sum_{j=-\lfloor (n+1)/2 \rfloor}^{\lfloor (n+1)/2 \rfloor} \hat{\beta}_n(j - \Delta/T) e^{-i\omega(j - \Delta/T)}}{\sum_{j=-n}^n \hat{\beta}_{2n+1}(j) e^{-i\omega j}}, \quad (17)$$

where the symbol $\lfloor \cdot \rfloor$ denotes the integer part of the real number and $\hat{\mathbf{B}}_n(\omega)$ is the Fourier transform of the function $\hat{\beta}_n(t)$ equal to:

$$\hat{\mathbf{B}}_n(\omega) = \frac{\sin(\omega/2)^{n+1}}{(\omega/2)^{n+1}}, \quad (18)$$

and where ω is a spatial frequency associated with the variable t ;

$$4) \quad H_0(\omega) \leq |H_\Delta(\omega)| \leq |H_{T/2}(\omega)|, \quad (19)$$

5) for large values of the degree n we have:

$$H_\Delta(\omega) \cong \frac{\mathfrak{G}_3(\pi(-\Delta + i(1+n)\omega T / 12), e^{-(1+n)\pi^2/6})}{\mathfrak{G}_3(\pi i(1+n)\omega T / 6, e^{-(1+n)\pi^2/3})}, \quad (20)$$

where $\mathfrak{G}_3(z, q) = \sum_{j=-\infty}^{\infty} q^{j^2} e^{2nij}$ is the elliptic Jacobi theta function;

$$6) \quad \lim_{n \rightarrow \infty} H_\Delta(\omega) = \begin{cases} 1 & \text{for } \omega < \pi / T, \\ 0 & \text{for } \omega > \pi / T, \end{cases} \quad (21)$$

$$7) \quad \lim_{n \rightarrow \infty} H_0(\pi / T) = 1, \quad (22)$$

$$H_{T/2}(\pi / T) = 0. \quad (23)$$

The proof of the Proposition is given in the Appendix.

Figure 2 shows plots of families of amplitude characteristics $|H_\Delta(\omega)|$ for different values of the degree n of the spline curve. We can see that the characteristics resemble a low-pass filter characteristic with the cutoff frequency $\omega_c = \pi / T$, and thus with the length $\lambda_c = 2T$.

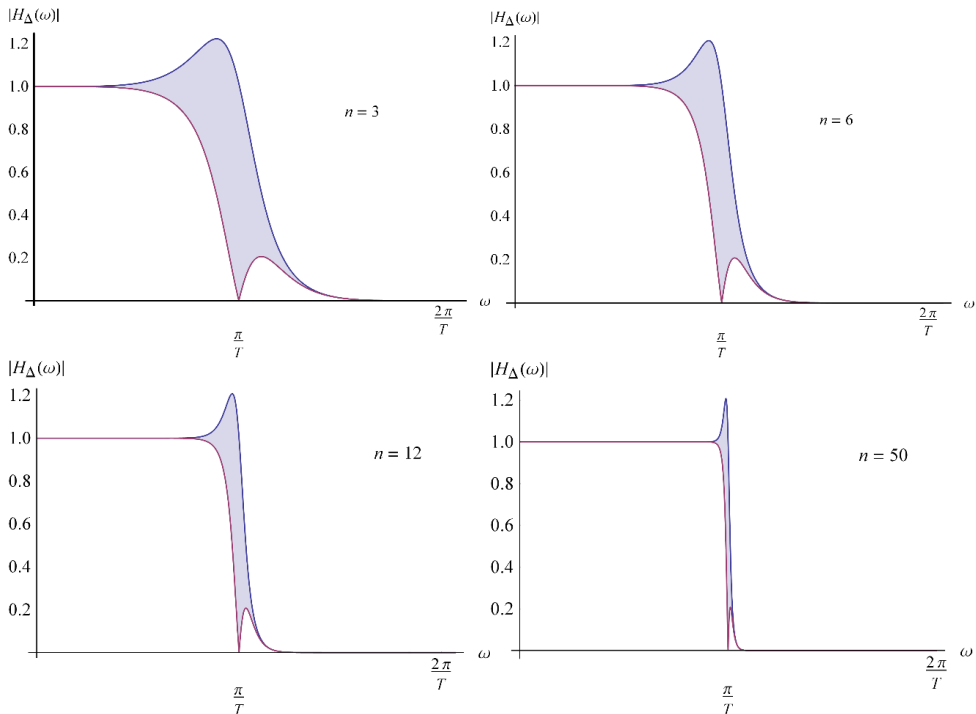


Fig. 2. Families of the filter amplitude characteristics for different filter orders.

Therefore, for the predetermined cutoff length λ_c , the distance between nodes of the spline function should be $\lambda_c / 2$. Note, that the higher the degree n , the better the approximation of

the ideal filter response. Obviously, one should realize that the higher the degree of the spline functions, the more numerically complex the filter becomes.

These properties seem surprising at first, because the higher the degree n of the B-spline function, the smoother the function. Accordingly, it appears that the cutoff frequency of the transfer function $H_{\Delta}(\omega)$ should decrease with increasing n . However, it is not the case here. This can be explained by simple reasoning. Consider a function:

$$f(t) = \sum_{k=-\infty}^{\infty} (-1)^k \beta_{n,T}(t - kT). \quad (24)$$

We can see that an increase in n causes that the function becomes more and more similar to a cosine function with the frequency $\omega = \pi / T$. Hence, we obtain (22). However, since $\beta_{n,T}(t)$ is an even function, it is clear that B-spline functions cannot be used to well approximate the sine function $\sin(\pi t / T)$, which is an odd function and has zero values at the nodes. Hence, we have (23).

2.3. Remarks on the numerical properties of the algorithm

To implement the algorithm, it is necessary to repeatedly determine the values of the shifted spline functions at the points with coordinates t_m . The amount of calculations one needs to perform can be reduced if the profile sampling interval Δt is constant and the distance between nodes of the spline function is a multiple of Δt . In this case, it is sufficient to tabulate the values of the B-spline basis function at the points with coordinates being the multiple of Δt . It is also important that, in order to make the matrix \mathbf{B} non-singular, the number of profile samples should not be smaller than the number of the parameters of approximation (8).

2.4. Comparing the spline filter with the filter based on B-spline function approximation

Both the classical spline filter and the filter described in Subsection 2.1 of this paper use the concept of minimization of the residual error (1). In the spline filter, an appropriate cutoff frequency is achieved by adding a certain penalty function to the functional (1), with the penalty function representing the bending energy of the filtered profile. As a result, the spline filter minimizes the functional:

$$J = \sum_{m=1}^M (x_m - s(t_m))^2 + \eta \int_0^{T_f} \left(\frac{d^p s(t)}{dt^p} \right)^2 dt. \quad (25)$$

The value of the coefficient η is selected in such a way, so as to achieve the desired cutoff wavelength. If the sampling period of the signal $x(t)$ is small enough, we can assume that [3]:

$$\eta = (\lambda_c / 2\pi)^{2p}. \quad (26)$$

The parameter p affects the slope of the filter amplitude characteristic in the filter transition band; the higher the value of p , the steeper the characteristic curve amplitude and the narrower the transition bandwidth.

In the paper by Krystek [1] and the respective standard [6] (with both considering the case of $p = 2$), the variational problem $\min_{s(t)} J$ is solved by approximating the continuous function $s(t)$ with the discrete sequence s_m , and then replacing the square integral of the derivative of the function $s(t)$ with the sum of squares of the properly defined difference quotient. On the

other hand, in [3], the function $s(t)$ is approximated by a linear combination of the shifted B-spline functions of the form (8). In this case, the distance between nodes of the B-spline function should be at least approximately six times smaller than the cutoff length λ_c in order to ensure sufficient accuracy of approximation of the function $s(t)$. Moreover, if continuity of the derivative $s^{(p)}(t)$ is to be achieved, the degree of the B-spline functions should not be lower than $p + 1$. Obviously, it is possible to use some other methods of approximation of the function $s(t)$, e.g. approximation by a linear combination of Legendre polynomials scaled in such a way, that they are orthogonal in the interval \mathcal{P} .

The filter described in Subsection 2.1 does not use the penalty function. Yet, the appropriate smoothness of the function $s(t)$ is achieved only by selecting a sufficiently high value of the distance T . From Property 6 of the Proposition it is clear that a filter with the cutoff wavelength λ_c can be obtained by assuming that $T = \lambda_c / 2$. It should be emphasized that the method of approximation of the function $s(t)$ based on B-spline functions described by (8) is really crucial here, because the proof of property (20), which results in (21), significantly exploits the fact that the base function $\hat{\beta}_n(t)$ used for the approximation resembles the Gaussian function, as shown in (6). The filter described in Subsection 2.1 is much simpler than the spline filter. There is no need to take into account the bending energy, and the number of parameters describing the filtered function is much smaller. This features are particularly important in two-dimensional filtering of surfaces.

One of the reasons for development of spline filters is to eliminate the end effect. In the problem of profile feature separation, the end effect occurs when the form component of the primary profile is much larger than the roughness component. Below, the two filters are compared in terms of end effect elimination using a simulation method. Let us consider a signal in the form:

$$x(t) = \cos 2\pi t / 3\lambda_c. \quad (27)$$

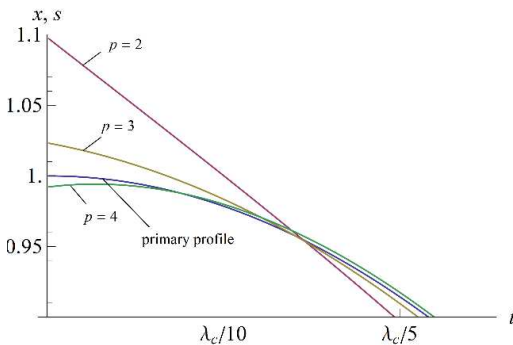


Fig. 3. The primary cosine signal and the signals filtered by the spline filter $p = 2, 3, 4$.

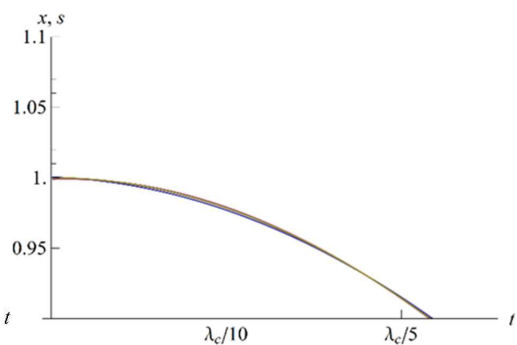


Fig. 4. The primary cosine signal and the signals filtered by the filter using the B-spline function approximation for $n = 2, 3$.

The signal consists of one wave with the length of $3\lambda_c$, which is significantly greater than the filter cutoff wavelength. Let us note that the highest value of the second derivative of the function (27) occurs along the edge for $t = 0$. Thus, the expected end effect should be the most visible. Fig. 3 shows, in the initial range of the variable t , the primary signal and the signals filtered with the spline filter for different values of the parameter p . It is clear that for $p = 2$ the

end effect is considerable and that the difference $s(0) - x(0)$ reaches 10% of the amplitude of the signal (27). This value is smaller than 1% only when $p = 4$. For this reason, the filter implementation described in [3] required using the B-spline function of the $n = 5$ degree. For comparison, Fig. 3 shows the effect of the operation of the filter using B-spline function approximation for $n = 2$ and $n = 3$. As can be seen, the filtered signals actually coincide with the primary signal. It turns out that as early as for $n = 2$ (quadratic splines) the difference $s(t) - x(t)$ does not exceed 1% in the whole interval of variation t .

2.5. An example of approximation of a 2D profile

To illustrate the performance of the approximation algorithm, let us determine, for example, a 2D roughness profile of the inner ring race of the 608 series ball bearing. Nominally, the race cross-section has the shape of a circle with the radius $r = 2.05$. Here, the spatial variable is denoted by x and the values of the profile by y . In Fig. 5, we can see the measured item. The surface topography was measured using a contact profile-meter with an adjustable table, which enables measurements of 2D and 3D profiles.



Fig. 5. The measured object.

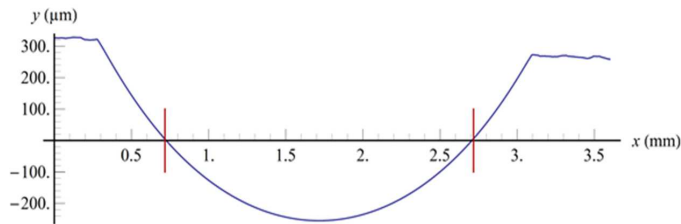


Fig. 6. Cross-section of the bearing race and limits of its central part.

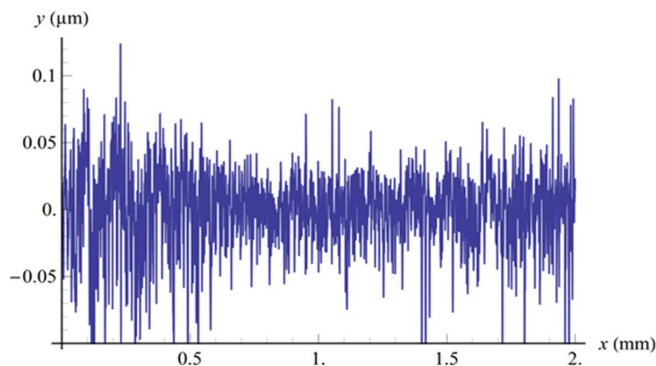


Fig. 7. The 2D roughness profile.

Figure 6 shows the measured profile of a cross-section of the bearing race. The profile was measured using the sampling interval $\Delta x = 1 \mu\text{m}$. Our objective was to determine the roughness of the central part of the profile, with the filter cutoff length being $\lambda_c = 0.25 \text{ mm}$, and the profile length $8\lambda_c$. The profile was approximated using cubic spline functions with the node-to-node distance $T = \lambda_c / 2$. Fig. 7 presents the roughness profile obtained by subtracting the measured profile from the approximated profile representing the mean line. We can see that the roughness profile was determined correctly; there was no end effect, despite the fact that the amplitude of the form component of the measured profile was a thousand times higher than the amplitude of the roughness component.

3. Approximation of periodic profiles

Periodic profiles appear in problems related to the measurement of roundness of rotary machine parts. Typically, it is assumed that a measured profile consists of a form profile, whose wave numbers range from 2 to 15, and a waviness profile with wave numbers in the range 15–500. The form and waviness are generally separated using Gaussian filters, and the filtration is performed usually in the domain of profile Fourier components. In the literature, other approaches are also met. In [2], for example, profiles are filtered by applying a variational approach, which leads to the so-called discrete spline filter for periodic profiles. In [13, 14] the filtration is based on a wavelet transform. This section presents a method that involves approximating profiles by means of periodic B-spline functions.

Periodic functions can be approximated and smoothed using periodic B-spline functions. We assume that, in periodic spline functions, their nodes are uniformly distributed over an interval $[0, 2\pi]$, thus $T = 2\pi / K$ for a certain positive integer K . The function:

$$\gamma_{n,K}(t) = \sum_{j=-\infty}^{\infty} \beta_{n,T}(t - 2\pi j) \quad (28)$$

is a periodic B-spline function with the period 2π and the node-to-node distance $T = 2\pi / K$. Note that, in practical applications, the condition $n + 1 < K$ is generally satisfied, thus:

$$\gamma_{n,K}(t) = \beta_{n,2\pi/K}(t) \text{ for } t \in [-\pi, \pi]. \quad (29)$$

A periodic spline function can be represented as a linear combination of periodic B-spline functions in the form:

$$s(t) = \sum_{k=0}^{K-1} a_k \gamma_{n,K}(t - 2\pi k / K) = \mathbf{a}^T \boldsymbol{\gamma}(t), \quad (30)$$

where:

$$\mathbf{a} = [a_0 \ a_1 \ \dots \ a_{K-1}]^T, \quad (31)$$

$$\boldsymbol{\gamma}(t) = [\gamma_{n,K}(t) \ \gamma_{n,K}(t - 2\pi / K) \ \dots \ \gamma_{n,K}(t - 2\pi(K-1) / K)]^T. \quad (32)$$

Periodic B-spline functions have properties similar to properties 1)–4) described in the previous section. The spatial frequency ω should only be replaced by the index of the component of the expansion of the function $s(t)$ into an exponential Fourier series κ (we use the following form of Fourier series: $x(t) = \frac{1}{2\pi} \sum_{\kappa=-\infty}^{\infty} X(\kappa) e^{i\kappa t}$). Thus, for example, the following formula is equivalent with that of the (17):

$$H_{\Delta}(\kappa) = \hat{B}_n(\kappa T) \frac{\sum_{j=-\lfloor (n+1)/2 \rfloor}^{\lfloor (n+1)/2 \rfloor} \gamma_{n,K}(jT - \Delta) e^{-i\kappa(jT - \Delta)}}{\sum_{j=-n}^n \gamma_{2n+1,K}(jT) e^{-i\kappa jT}}. \quad (33)$$

On the other hand, properties 5) and 6) do not occur, because the function $\gamma_n(t)$ does not converge to the Gaussian function, when $n \rightarrow \infty$.

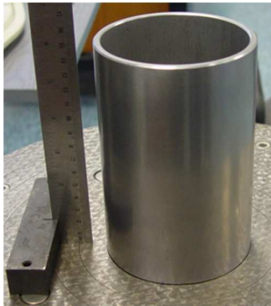


Fig. 8. The measured object.

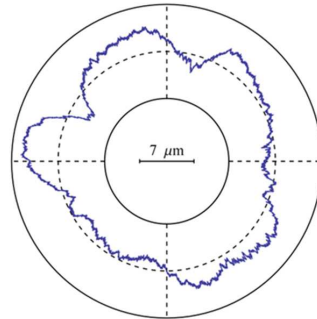


Fig. 9. The profile measured in a selected cross-section.

Let us discuss an example of the application of the algorithm to approximate a roundness profile. The measurement was performed using a modernized Taylor Hobson Talycenta, which is an instrument with a rotary table for measuring roundness and cylindricity profiles. The measured object was a hollow cylinder with the outer radius $R = 140$ mm, shown in Fig. 8. In the instrument, the profile sampling is synchronized with the encoder of the measuring table, which gives 4096 samples per revolution. In Fig. 9, we can see a profile of the cylinder cross-section. Now, the spatial variable is an angular variable denoted by ϕ , and the profile height is denoted by r . The form profile is determined by approximating the profile using periodic cubic B-splines. It was assumed that the index of the cutoff wave is $\kappa_c = 15$, which gives $K = 30$ B-splines.

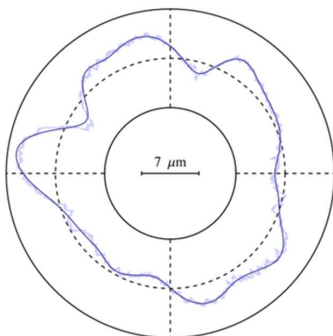


Fig. 10. The form of the measured roundness profile.

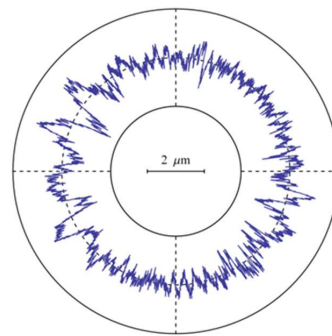


Fig. 11. The waviness of the measured roundness profile.

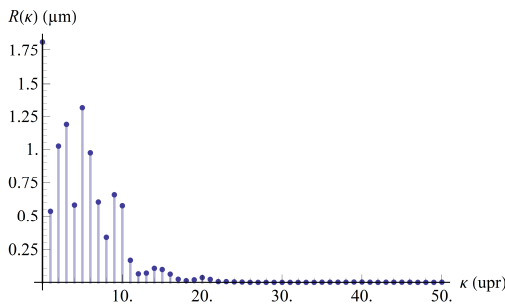


Fig. 12. The amplitudes of the harmonics of the form component.

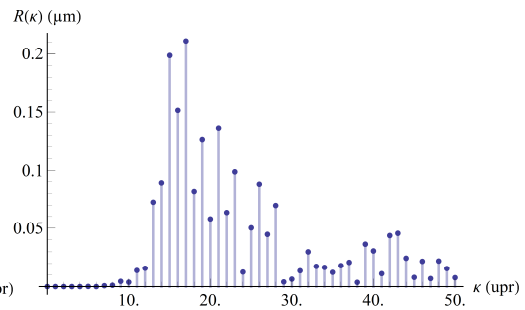


Fig. 13. The amplitudes of the harmonics of the waviness component.

Figures 10 and 11 show the separated form and waviness of the measured roundness profile. In Figs. 12 and 13 we can see the respective amplitudes of their harmonics. In the form component, waves with the number of undulations per rotation (upr) smaller than 15 are predominant. In the waviness component, on the other hand, there are mainly waves with the number of upr greater than 15. Waves with upr close to 15 occur in both components. Obviously, if a filter with a higher degree of the B-spline function is used, the separation of the two components will be better.

4. Conclusion

The study aimed at developing a method for approximation of the measurement data for non-periodic and periodic 2D profiles using B-spline functions. Acceptable smoothness of lines and surfaces was achieved by selecting an appropriate distance between nodes of the spline function. It was shown that the node-to-node distance of the spline should be equal to half of the desired cutoff length of the filter. Moreover, it is possible to obtain an arbitrarily large inclination of the frequency characteristic in the transition band if a sufficiently high degree of the spline function is selected.

The paper includes examples of separation of 2D roughness by means of the developed approximation method using B-spline functions. The experiments show that a roughness profile can be determined correctly, without any end effect, even if the amplitude of the form component of a measured profile is very much higher than the amplitude of the roughness component. The paper also includes examples of separation of form and waviness of roundness profiles.

A certain shortcoming of the filter based on approximation of spline functions is the fact that it is spatially-varying. Furthermore, the frequency characteristic of a two-dimensional filter is not circularly invariant, which might be essential when isotropic surfaces are analyzed. These two drawbacks can be eliminated by extending the functional defining the filter parameters with an appropriate bending energy of a spline line or surface. However, the distance between nodes of the spline function needs to be smaller then. The filter can be approximately spatially-invariant and circularly invariant when the node-to-node distance is about five to six times smaller than the desired cutoff lengths [3, 15]. This results in greater complexity of the filter. In this sense, the developed algorithm is simple – it ensures appropriate smoothness of the lines and surfaces at a small number of B-spline basis functions.

Appendix

The properties 1 and 2 are obvious. Let us prove the property 3. The Fourier transform of the spline function $s(t)$ is:

$$S(\omega) = \sum_{k=-\infty}^{\infty} a_k \mathcal{F}[\beta_{n,T}(t-kT)] = \sum_{k=-\infty}^{\infty} a_k \hat{B}_n(\omega T) e^{-i\omega kT} = \hat{B}_n(\omega T) A(\omega T), \quad (34)$$

where $A(\omega T)$ is a discrete Fourier transform of the sequence $\{a_k\}$. Setting the partial derivative of the functional J with respect to the coefficient a_k to zero, we obtain:

$$\begin{aligned} \frac{1}{2} \frac{\partial J}{\partial a_k} &= - \int_{-\infty}^{\infty} \beta_{n,T}(t-kT) \left(x(t) - \sum_{j=-\infty}^{\infty} a_j \beta_{n,T}(t-jT) \right) dt \\ &= - \int_{-\infty}^{\infty} \beta_{n,T}(t-kT) x(t) dt + \sum_{j=-n}^n a_j \beta_{2n+1,T}((j-k)T) = 0. \end{aligned} \quad (35)$$

(Here we used the property $\beta_{2n+1,T}(t) = \beta_{n,T}(t) * \beta_{n,T}(t)$ and the fact that $\beta_{2n+1,T}(t) = 0$ for $t \geq nT$). Assume that $x(t) = \delta(t - \Delta)$. Then, from the above equation, it follows:

$$\sum_{j=-n}^n a_j \beta_{2n+1,T}((j-k)T) = \beta_{2n+1,T}(\Delta - kT), k = \dots, -1, 0, 1, \dots \quad (36)$$

Determining the discrete Fourier transform of both sides of the (36) treated as sequences with respect to index k , we obtain:

$$\sum_{j=-n}^n \beta_{2n+1,T}(jT) e^{-i\omega Tj} A(\omega T) = \sum_{j=-\lfloor (n+1)/2 \rfloor}^{\lfloor (n+1)/2 \rfloor} \beta_{n,T}(jT - \Delta) e^{-i\omega Tj}. \quad (37)$$

The Fourier transform of the impulse $x(t) = \delta(t - \Delta)$ is equal to $e^{-i\omega \Delta}$. Hence, and from the (34) and (37), we obtain (17). The property 4 can be easily proven for particular values of n . For example, when $n = 3$, the derivative of square root of the absolute value of the numerator of the fraction in (17) with respect to Δ is:

$$-\frac{8}{3T^8} \Delta(T - \Delta)(T - 2\Delta) \left(T^2 + \Delta(T - \Delta)(1 - \cos \omega T) \right) \sin^2 \omega T. \quad (38)$$

It is easy to prove that if $\Delta < T/2$, then the above expression is negative. Thus, the expression $|H_{\Delta}(\omega)|$ decreases with respect to Δ for $0 < \Delta < T/2$. The property 5 results from (6). The author does not know a proof of the properties 6 and 7. They have been checked only numerically (Fig. 2). For instance, when $n = 10$, we obtain:

$$H_0(\pi/T) = \frac{1389257839119150}{4722116521\pi^{11}} = 0.999994. \quad (39)$$

References

- [1] Krystek, M. (1996). Form filtering by splines. *Measurement*, 18(1), 9–15.
- [2] Krystek, M. (1996). Discrete L-spline filtering in roughness measurements. *Measurement*, 18(2), 129–138.
- [3] Janecki, D. (2013). A two-dimensional isotropic spline filter. *Prec. Eng.*, 37(3), 948–965.
- [4] Seewig, J. (2005). Linear and robust Gaussian regression filters. *J. Phys. Conf. Ser.*, 13, 254–257.

- [5] Brinkmam, S., Bodschwinna, H., Lemke, H.W. (2001). Accessing roughness in three-dimensions using Gaussian regression filtering. *Int. J. Machine Tools Manuf.*, 41(13–14), 2153–2161.
- [6] ISO/TS 16610-22:2006. Geometrical Product Specifications (GPS) – Filtration – Part 22, Linear Profile Filters, Spline Filters.
- [7] ISO/TS 16610-31:2010. Geometrical product specifications (GPS) – Filtration – Part 31, Robust profile filters, Gaussian regression filters.
- [8] Dobrzanski, P, Pawlus, P. (2010). Digital filtering of surface topography. Part I. Separation of one-process surface roughness and waviness by Gaussian convolution, Gaussian regression and spline filters. *Prec. Eng.*, 34(3), 647–50.
- [9] Zhang, H., Yuan, Y., Piao, W. (2010). A universal spline filter for surface metrology. *Measurement*, 43(10), 1575–1582.
- [10] Hanada, H., Saito, T., Hasegawa, M., Yanagi, K. (2008). Sophisticated filtration technique for 3D surface topography data of rectangular area. *Wear*, 264(5–6), 422–427.
- [11] Schoenberg, I.J. (1969). Cardinal interpolation and spline functions. *J. Approx. Theory*, 2(2), 167–206.
- [12] Unser, M., Aldroubi, A., Eden, M. (1993). B-spline signal processing. Part I – Theory. *IEEE Trans. Signal Processing*, 41(2), 821–848.
- [13] Adamczak, S., Makiela, W. (2011). Analyzing variations in roundness profile parameters during the wavelet decomposition process using the Matlab environment. *Metrol. Meas. Syst.*, 18(1), 25–34.
- [14] Stępień, K., Makiela, W. (2013) An analysis of deviations of cylindrical surfaces with the use of wavelet transform. *Metrol. Meas. Syst.*, 20(1), 139–150.
- [15] Janecki, D. (2009). A generalized L2-spline filter. *Measurement*, 42(6), 937–943.